# Solidlike and liquidlike behavior in monolayers and multilayers of metal-bearing amphiphiles

Smita Mukherjee,[1] Alokmay Datta,[1,*] Angelo Giglia,[2] Nicola Mahne,[2] and Stefano Nannarone[2,3]
[1]*Applied Material Science Division, Saha Institute of Nuclear Physics, 1/AF Bidhannagar, Kolkata 700 064, India*
[2]*TASC-INFM National Laboratory, Area Science Park, Basovizza (Trieste), Italy*
[3]*INFM and Dipartimento di Ingegneria dei Materiali ed Amb., Università di Modena e Reggio Emilia, Italy*
(Received 2 May 2011; revised manuscript received 19 July 2011; published 29 August 2011)

Atomic force microscopy (AFM) of cadmium stearate (CdSt) and cobalt stearate (CoSt) Langmuir-Blodgett films show differences in their in-plane morphologies. CdSt films, with a huge number of in-plane "pinhole" defects, follow self-affine behavior, whereas CoSt films, which are almost void of such in-plane defects, show deviation from self-affinity especially at small length scales, suggesting liquidlike behavior, imparting flexibility to the system, in plane. Phase images of CoSt obtained from tapping mode AFM show gentle undulations or hemispherelike features in contrast to its smooth topography, unlike the CdSt system where both height and phase images show self-affine domains. Near edge x-ray absorption fine structure spectroscopy indicates no preferred in-plane orientation of the head group in CoSt films. The undulating features in CoSt is explained by invoking a radially symmetric orientational distribution in the tilt of adjacent hydrocarbon tails, causing a small in-plane density variation which shows up in the phase image. These orientational disorders in adjacent tails probably allow "filling up" of in-plane defects thereby giving rise to its excellent in-plane coverage and hence a "liquidlike" behavior in CoSt. Brewster angle microscopy shows that parent Langmuir monolayers of stearic acid in the presence of Cd and Co ions in the aqueous subphase behave as two-dimensional "solids" and "liquids," respectively, suggesting the phenomena to be inherent in the amphiphiles and probably independent of their organization as monolayers and multilayers.

DOI: 10.1103/PhysRevE.84.021606 PACS number(s): 68.47.Pe, 68.37.Ps, 68.18.−g, 68.35.Ct

## I. INTRODUCTION

The standard structural distinctions of isotropy and lack of long-range order in liquids [1] are not valid for complex liquids in general, and for amphiphilic materials in particular [2]. In the latter, on the one hand, the differences in interaction between the nonpolar hydrocarbon chains (short-range) and the polar "head groups" (long-range) can give rise to different two-dimensional positionally ordered phases with correlation length dependent on density and temperature, and on the other hand, the "rodlike" molecules can lead to different orientationally ordered phases. Extensive studies on amphiphilic monolayers on water surface have looked at both these aspects and have established a connection between bond ordering and orientational ordering of the chains, and positional ordering of the molecules [3–5].

In these two-dimensional systems, there are two ways of distinguishing a liquid from a solid. The first has to do with bond orientational order in the "lattice" of the constituents, be they atoms, molecules, clusters, holes, or vortices. Here, the long-range bond orientational order in the hexagonal lattice denotes the hexatic phase [1] while this order is broken in the liquid phase by the passage to randomly distributed polygonal arrangements [6]. As the microscopic order in solids is manifested in the occurrence of cleavage planes and grains in their breakdown, this randomness in microscopic bonding is coarse-grained into randomly connected holes or bubbles in complex liquids such as soap films [1,7]. The second distinction comes from the presence of a uniform surface tension on a liquid surface in equilibrium, which responds to strain at any length scale by dissipating this strain through capillary waves. Hence the liquid surface is characterized by capillary waves causing height fluctuations of any wavelength within the range defined by molecular size and sample size which leads to a logarithmic height correlation with the in-plane separation [8], without any cutoff. This contrasts with the self-affine height correlation with an explicit "correlation length" or cutoff and an algebraic dependence on the in-plane separation [8], observed in solid surfaces.

While most of the studies of height correlations in amphiphilic monolayers on water surface have been carried out on pristine amphiphiles such as long chain fatty acids [9] with some exceptions [10,11], how the presence of counterions, in particular, specific divalent metal ions, in the water modifies these correlations is far from clear. On the other hand, since only divalent metal-bearing amphiphilic fatty acids form stable multilayers [12], height correlation studies have been carried out on these only. To be more specific, multilayers of only cadmium salts of these fatty acids have been studied thoroughly [13–15]. Both these Langmuir monolayer and Langmuir-Blodgett multilayer studies show that they have liquidlike height correlation when the observation area is large [9–11,13–15] while the multilayers exhibit self-affine correlation over small scan lengths [14,15]. However, there is little information about what happens in the multilayers when the metal is changed as also any connection between the liquidlike or solidlike behavior of the metal-bearing amphiphilic monolayer on water and the height correlations obtained in the multilayers on solid substrates of the same amphiphile.

In our previous reports, we have shown that the coordination and hence the geometry of the metal-carboxylate head group decides the presence or absence of long-range intermolecular forces through the presence or absence of dipole moment, and this may control the liquidlike or solidlike behavior of

*alokmay.datta@saha.ac.in

 

the corresponding multilayers [16]. In this communication we compare the height correlations in monolayers and multilayers of amphiphilic salts of two different divalent metals, Cd and Co, deposited on amorphous substrates to bring out their essential differences as "solidlike" or "liquidlike," respectively. We have further shown the continuity of these behaviors in the parent Langmuir monolayers to suggest the inherent molecular basis of these behaviors.

## II. EXPERIMENTAL DETAILS

One and three monolayers (MLs) each of cadmium stearate (CdSt) and cobalt stearate (CoSt) were deposited on hydrophilic silicon (100) substrate by the Langmuir-Blodgett (LB) technique [12]. For this, respective divalent metal ions (i.e., $Cd^{2+}$ and $Co^{2+}$) were introduced in a Langmuir trough (KSV instruments, KSV-5000) containing Milli-Q water (resistivity 18.2 MΩ cm) by addition of 0.5 mM chloride solutions of these. Subphase *p*H was maintained at 6.0 by adding sodium bicarbonate ($NaHCO_3$, Merck, 99%). Stearic acid ($C_{17}H_{35}COOH$, Sigma-Aldrich, 99%) solution (0.5 mg/ml) was spread to form the monolayer. Silicon substrates used for film deposition were hydrophilized by keeping them in a solution of ammonium hydroxide (Merck, 98%), hydrogen peroxide (Merck, 98%), and Milli-Q water ($H_2O$:$NH_4OH$:$H_2O_2$ 2:1:1 by volume) for 10–15 min at 100°C. Films were deposited at a monolayer pressure of 30 mN/m at 19°C at a dipping speed of 3 mm/min by subsequent up-down strokes of the substrate through the air-water interface, the first layer being deposited by an upstroke of the substrate from water to air through the interface. Drying time after first stroke was 10 min. Films were checked for reproducibility. Atomic force microscopy (AFM) was performed in tapping mode using Nanoscope IV, VEECO Inc. with a silicon cantilever (force constant 40 N/m). Scans were performed over several regions of the films for different scan areas. Near edge x-ray fine structure (NEXAFS) spectroscopy [17] at oxygen *K* edge (∼530 eV) was carried out at normal and grazing incidence using synchrotron radiation at BEAR beamline, ELETTRA synchrotron. The spectra were recorded by total electron yield (TEY). They were normalized to an $I_0$ spectrum previously measured for clean copper to account for oxygen in mesh. Monochromator slits (50 μm) were set to provide an energy resolution of 0.1 eV. Brewster angle microscopy (BAM) using an imaging ellipsometer (Accurion GmbH, EP3) with no compensator and incident angle at 53° (Brewster angle for water) and with 10× magnification was employed to study the morphology of parent Langmuir monolayers of stearic acid in the presence of Cd and co ions in subphase present in the same concentration at which LB films have been lifted. BAM images were taken during decompression of the barriers in order to understand the disassembling behavior of the films at the air-water interface.

## III. RESULTS AND DISCUSSION

### A. Solidlike and liquidlike LB films: An AFM study

*Surface morphology and height-height correlation.* AFM topographic images of 1 ML [scan size (*S*): $1 \times 1$ $\mu m^2$] and 3 ML (*S*: $5 \times 5$ $\mu m^2$) films of CdSt and CoSt are shown in Fig. 1. As seen from the topographic images of the CdSt films, both 1 ML [Fig. 1(a)] and 3 ML [Fig. 1(c)], show the presence of a large number of in-plane "pinhole" defects, compared to the almost defect-free topography of CoSt [1 ML, Fig. 1(b) and 3 ML, Fig. 1(d)]. Specifically, it must be mentioned here that although the 1 ML CdSt film has been formed by passing the substrate through the monolayer once (hence the nomenclature), the same after deposition shows features of a trilayer film. As reported previously [16,18], the CdSt and CoSt films resemble two different growth modes [19], viz., the Volmer-Weber (V-W) or island type for the former and Frank van der Merwe (F-M) or wetting type in the case of the latter. Although these growth modes relate to the out-of-plane growth of the films, they are dependent on the formation of pinhole defects in this type of LB film [20], the latter also deciding the in-plane growth or surface morphology. Now, all rough surfaces exhibit perpendicular fluctuations, which are characterized by a mean-square roughness $\sigma = \overline{h(x_0,y_0)^2}^{1/2}$, $h(x_0,y_0) = h_0(x_0,y_0) - \overline{h_0(x_0,y_0)}$, where $h_0(x_0,y_0)$ is the height fluctuation at any point $(x_0,y_0)$ and the overbar denotes spatial average over a planar rough surface [21,22]. The roughness is termed "Gaussian" if $h(x_0,y_0) - h(x',y')$ is a Gaussian random variable whose distribution depends only on the relative coordinates $(x,y) = (x' - x_0, y' - y_0)$. For any isotropic Gaussian rough surface, the mean-square surface fluctuation is given by

$$g(r) = \langle [h(x + x_0, y + y_0) - h(x_0,y_0)]^2 \rangle, \qquad (1)$$

where $r^2 = (x^2 + y^2)$; the average is taken over all pairs of points on the surface which are separated horizontally by the length *r*, with $\langle\ \rangle$ denoting an ensemble average over all possible roughness configurations. In order to study

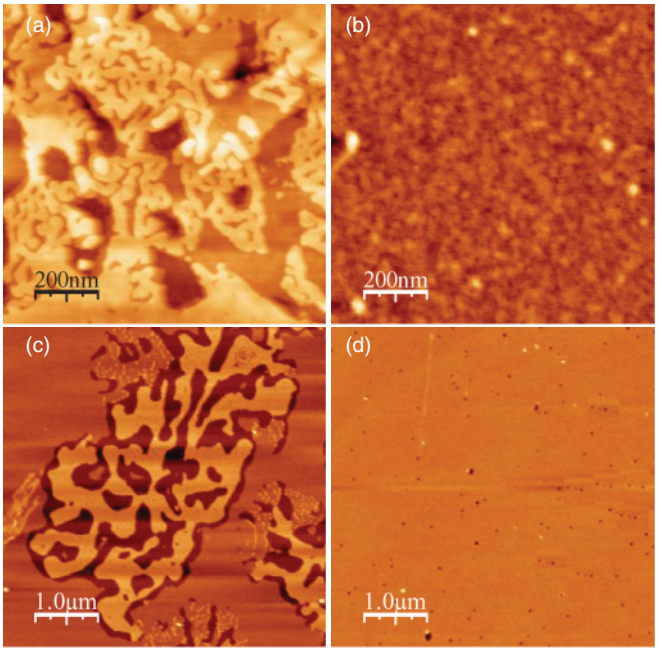


FIG. 1. (Color online) AFM topographic images of [(a),(b)] 1 ML ($1 \times 1$ $\mu m^2$) and [(c),(d)] 3 ML ($5 \times 5$ $\mu m^2$) films of [(a),(c)] CdSt and [(b),(d)] CoSt.

TABLE I. Conversion factor.

| Scan size ($\mu$m) | $m$ | $r$ (nm) |
|---|---|---|
| 0.2 | 1 | 0.78 |
| 0.5 | 1 | 1.95 |
| 1.0 | 1 | 3.91 |
| 2.0 | 1 | 7.81 |
| 5.0 | 1 | 19.53 |
| 10.0 | 1 | 39.06 |

the difference in surface morphology of the two types of metal-bearing films, this height-difference correlation function $g(r)$ was calculated from the AFM topographic images for various scan sizes for 1 and 3 ML films of CdSt and CoSt. To plot curves of different scan sizes in a single graph, instead of $g(r)$ vs $r$, we have plotted curves of $g(m)$ vs $m$, where $m$ stands for the number of pixels in the AFM image. For a particular scan size, one pixel corresponds to a specific value of the length $r$ in nm, the conversion factor being given in Table I. The $g(m)$ vs $m$ curves are plotted for CdSt [Figs. 2(a) and 2(c) for 1 and 3 ML films, respectively] and CoSt [Figs. 2(b) and 2(d) for 1 and 3 ML films, respectively] corresponding to different scan sizes [viz., (I) 0.5, (II) 1.0, and (III) 2.0 $\mu$m$^2$]. For the 3 ML films, the same are also plotted for 5.0 and 10.0 $\mu$m$^2$ scan sizes (inset).

If the surface exhibits self-affine roughness, $g(r)$ will scale as $g(r) \propto R^{2H}$, where $H$ is called the "roughness (Hurst) exponent." The mean-square roughness of any physical self-affine surface will saturate at sufficiently large lengths in plane. It is characterized by a correlation length $\xi$ such that

$$r \ll \xi, \quad g(r) \propto R^{2H}$$
$$r \gg \xi, \quad g(r) = 2\sigma^2,$$

where $\sigma$ is the saturation roughness.

A self-affine rough surface is characterized by the height-difference correlation function of the form [21]

$$g(r) = 2\sigma^2\{1 - \exp[-(r/\xi)^{2H}]\}, \tag{2}$$

The curves for CdSt and CoSt were fit with Eq. (2) and the parameters of fit are given in Table II. As seen

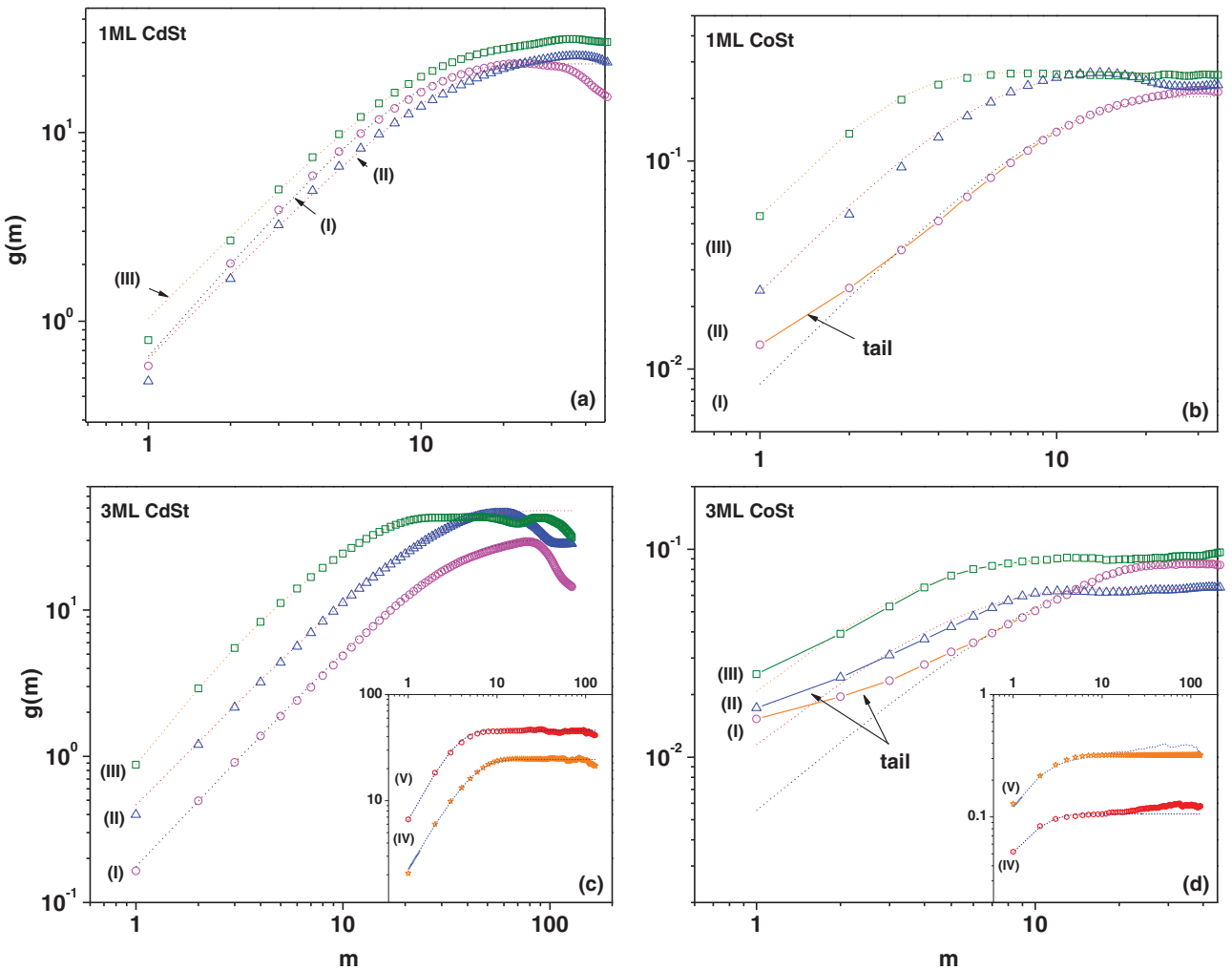


FIG. 2. (Color online) Height-difference correlation function of [(a),(b)] 1 ML and [(c),(d)] 3 ML films of [(a),(c)] CdSt and [(b),(d)] CoSt for (I) 500 × 500 nm$^2$; (II) 1 × 1 $\mu$m$^2$; (III) 2 × 2 $\mu$m$^2$; (IV) 5 × 5 $\mu$m$^2$; and (V) 10 × 10 $\mu$m$^2$ scan size. The symbols represent the data estimated from AFM topographic images, while the dotted lines are the fit corresponding to Eq. (2).

TABLE II. Parameters of fit with Eq. (2).

| | | CdSt | | | CoSt | | |
|---|---|---|---|---|---|---|---|
| Film | Scan size ($\mu$m) | $\sigma$ (Å) | $\xi$ (nm) | $H$ | $\sigma$ (Å) | $\xi$ (nm) | $H$ |
| 1 ML | 0.5 | 34.0 | 4.4 | 0.83 | 0.32 | 4.6 | 0.72 |
| | 1.0 | 35.0 | 2.8 | 0.76 | 0.36 | 1.2 | 0.75 |
| | 2.0 | 39.3 | 1.3 | 0.74 | 0.37 | 0.3 | 0.84 |
| 3 ML | 0.5 | 39.0 | 15.9 | 0.75 | 2.1 | 5.6 | 0.57 |
| | 1.0 | 49.0 | 6.4 | 0.72 | 1.8 | 1.1 | 0.57 |
| | 2.0 | 47.3 | 1.4 | 0.78 | 2.1 | 0.4 | 0.60 |
| | 5.0 | 35.0 | 0.3 | 0.78 | 2.3 | 0.1 | 0.60 |
| | 10.0 | 48.0 | 0.1 | 0.85 | 4.0 | 0.1 | 0.57 |

from the figures, curves for 1 and 3 ML CdSt [Figs. 2(a) and 2(c), respectively] show excellent fits to Eq. (2) and hence they strictly follow self-affine behavior for all length scales. We would like to mention here that this is consistent with previous results regarding height correlations obtained in CdSt films obtained from AFM measurements [13,14]. However, the height correlations obtained from diffuse x-ray scattering, which covers a much larger length scale, deviate from self-affinity even for CdSt films and show a liquidlike behavior [14,23,24]. The 1 and 3 ML CoSt curves, on the other hand, deviate from Eq. (2) [Figs. 2(b) and 2(d), respectively] at small $r$ and are fit separately (discussed below). Nevertheless, CoSt films obey self-affine nature at large length scales and hence, a comparison of the fitting parameters of Eq. (2) for CdSt and CoSt are discussed. As seen from Table II, the r.m.s. roughness $\sigma$ is considerably more for CdSt compared to CoSt for both the monolayer and trilayer films for all scan sizes, thereby indicating that the CoSt surface has a smooth morphology with negligible height variation. This is consistent with our previously reported results regarding the excellent out-of-plane growth of these type of films [20]. Moreover, as seen in Table II, in CoSt, the correlation length $\xi$ falls faster to zero than in CdSt, for all scan sizes, both for the 1 and 3 ML films.

The Hurst exponent $H$ is found to considerably decrease from ~0.8 to ~0.6 in going from the 1 ML CoSt to the 3 ML CoSt film in contrast to the constant value ~0.8 in the case of CdSt films. $H$ is related to the fractal dimension $D$ as $D = d - H$, where $d$ is the dimensionality of the system [24]. For thin films, where the height variations are orders of magnitude less than the in-plane surface coverage, $d\sim 2$. In such a case, for a V-W surface, $D < 1.5$ so that $H > 0.5$ and for an F-M surface, $D > 1.5$, so that $H < 0.5$. The $H$ values obtained in our case (Table II), consistent with our previous results [18], not only indicate this trend but also show that in the case of CoSt, in going from the 1 to the 3 ML film, the effect of substrate is reduced and that two-dimensional layering becomes more pronounced.

As mentioned earlier, the CoSt curves do not strictly obey self-affinity. Deviation from self-affinity is evident for $S =$ 500 nm for the 1 ML film. The effect is somewhat enhanced for the CoST trilayer, at lower scan sizes, viz., 0.2, 0.5, and 1.0 $\mu$m$^2$, all of which show teh presence of a "tail" (Fig. 3), a clear deviation from self-affine behavior. The tails are

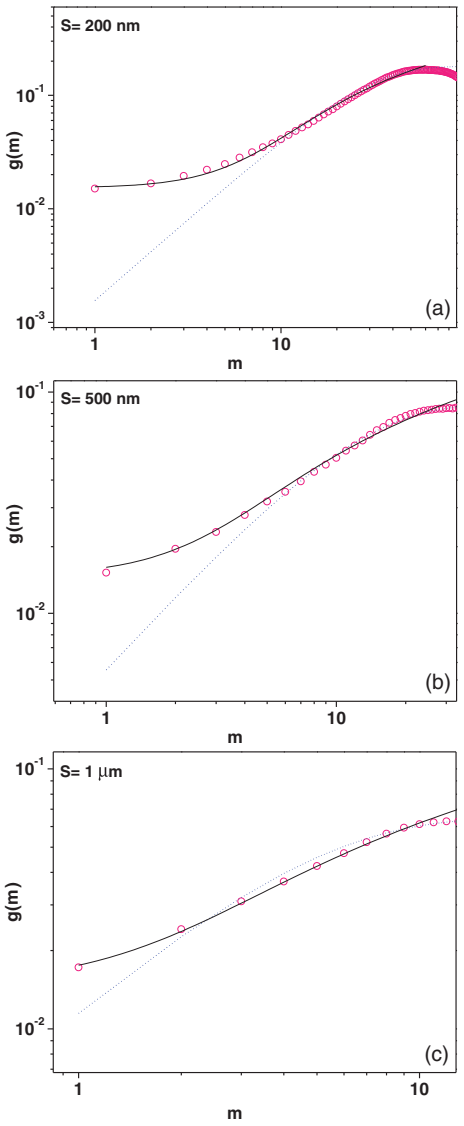


FIG. 3. (Color online) Height-difference correlation function of 3 ML CoSt films for (I) 200 × 200 nm$^2$; (II) 500 × 500 nm$^2$; and (III) 1 × 1 $\mu$m$^2$ scan size. The symbols represent the data estimated from AFM topographic images, while the dotted lines are the fit corresponding to Eq. (3).

separately fitted by a logarithmic function $f(r)$ of the form

$$f(r) = dln(ar^2 + br + c), \tag{3}$$

where $a$, $b$, $c$, and $d$ are parameters of fit (Table III). Although a logarithmic dependence is also observed for capillary waves generated on a liquid surface [8,13], it has a linear dependence on $r$ along with some constant. Our equation, however, contains a term quadratic in $r$, the coefficient of which is probably related to the areal number density, and a linear term in $r$ with a coefficient related to the wave number of the capillary waves, $c$ and $d$ being two constants involved with self-correlation. The values of these parameters show that with an increase in scan size, the $r^2$ term becomes more dominant, while the parameter $b$ remains more or less constant. Although it is not possible to give a detailed description of this function at this point, we have tried to relate this dependence

TABLE III. Parameters of fit with Eq. (3).

| Scan size ($\mu$m) | $a$ (nm$^{-2}$) | $b$ (nm$^{-1}$) | $c$ | $d$ (nm$^2$) |
|---|---|---|---|---|
| 0.2 | 0.009 | −0.001 | 1.343 | 0.052 |
| 0.5 | 0.150 | 0.050 | 2.250 | 0.018 |
| 1.0 | 0.450 | 0.050 | 2.500 | 0.016 |

to the observed density variation, discussed later in this paper. Nevertheless, this logarithmic dependence [14] as well as the absence of long-range intermolecular forces in CoSt films [16], suggest a probable liquidlike behavior in CoSt films in addition to self-affinity (at larger length scales).

It must be mentioned here that although the deviation from self-affinity is observed for small scan sizes, our results do not suggest that the effect is completely lost at large scan sizes but rather is masked due to an increase in the number of pinholes (although still very few compared to its CdSt counterpart). This deviation from self-affinity especially at small length scales is significant and indicates the difference in the microscopic organization of the metal-bearing amphiphiles. Again, that the effect is found to be enhanced for the 3 ML films from the 1 ML film is consistent with the idea that the liquidlike behavior is an inherent characteristic of the amphiphiles and is suppressed to an extent by interaction with hydrophillic substrate.

*Density variation on multilayer surface.* The difference between the films of these two metal-bearing amphiphiles becomes more stark if we compare the topographic and phase images of 3 ML films of CdSt [Figs. 4(a) and 4(b), respectively] and CoSt [Figs. 4(c) and 4(d), respectively] obtained from the tapping mode of AFM. CoSt phase image shows the presence of prominent "hemisphere-shaped" features all over the film covered surface, which are near absent in its corresponding topographic image. Against this, in CdSt at regions of full coverage, the phase image does not show such prominent "hemispheres" and both topographic and phase images show similar, "islandlike" features. This suggests the presence of a gentle undulation over the film covered surface in CoSt, which clearly does not arise due to interfacial roughness between two adjacent layers along $z$. The small r.m.s. roughness and also our previous results [16,20] suggest that successive LB multilayers of this type have smooth interfaces and hence do not affect the top roughness of the film covered surface. Thus a likely origin of such undulations in CoSt is in-plane density variation in the hydrocarbon chains. We suggest that this density variation (observed in the nm length scale) is the result of a radially symmetric orientational disorder in the tilt of the hydrocarbon tails in CoSt. Although an individual molecular tilt does not give rise to significant density change at that length scale, the same occurring in a radially symmetric manner and over a considerable area (∼nm) may cause an appreciable variation in density. This can be explained by considering two cylinders of volume $V$, each containing $N$ molecules, having radius $R_0$ and height $S_0$ (height of untilted molecular layer), placed adjacent to each other. The density then corresponds to the density of untilted molecules given by $\rho = N/V$. Next we consider that the molecules in the cylinders are tilted by angle $\theta$ in a radially symmetric fashion such that the cylinders take the shape of two frusta of radius $R$ such that $R > R_0$ for the first and $R < R_0$ for the second (Fig. 5), $h$ being the height of both frusta. The change in density $\Delta\rho$ is then given by

$$\Delta\rho = \frac{18a}{\cos\theta[9 - 3a^2 + a^4]}\rho, \tag{4}$$

where $a = (S_0/R)\sin\theta$. Assuming $S_0 = 5$ nm to be the typical bilayer height and $R = 25$ nm to be the radius of hemispheres observed in the AFM phase image, we plotted the variation of the percentage change in density with tilt angle $\theta$ (Fig. 6). We find that even for small amounts of tilt (∼20°), the percentage variation is appreciable (∼20%).

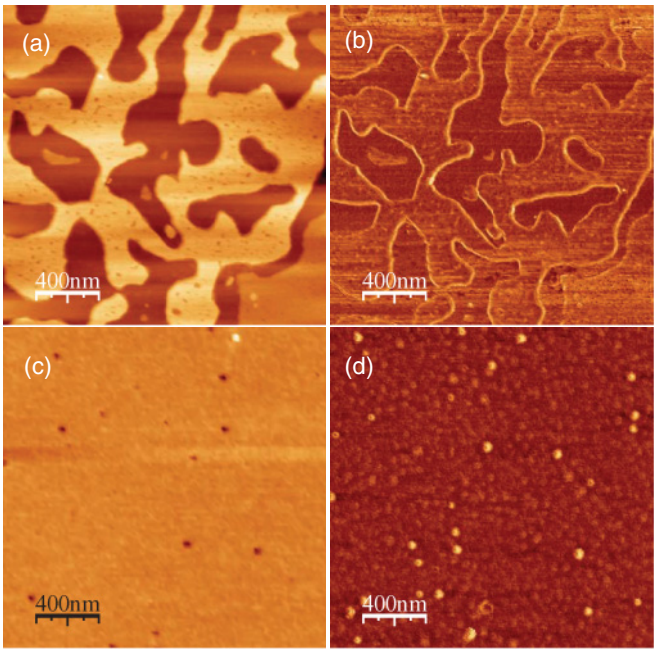


FIG. 4. (Color online) AFM images (2 × 2 $\mu$m$^2$) of 3 ML films of [(a),(b)] CdSt and [(c),(d)] CoSt, where [(a),(c)] and [(b),(d)] represent topographic and phase images, respectively.

It must be noted here that there is no relative height difference between the two cylinders or the two frusta, showing that the radially symmetric tilt of molecules by an angle $\theta$ do not contribute to any height variation. However, within any particular frustum whose radius $R > R_0$, there are a large number of concentric frusta with tilt angles varying from 0 to $\theta_{\max}$. This tilt variation leads to a small height variation [Fig. 5 (inset)], which becomes prominent only for small scan sizes and gets masked when pinholes become dominant in a system. We propose that in the case of CoSt, for small scan size (where pinhole defects are insignificant), the AFM tip senses both the height and density variation arising due to molecular tilt. In the height image, they manifest themselves as tails and in the phase image they emerge as the hemisphere-like features. We find that $1/b$, where $b$ is the coefficient of the linear term of Eq. (3), has a value ∼20 nm, which is of the order of the average radius $R$ of the hemispheres. The first term of Eq. (3) probably gives the total number of such correlated frusta with $R > R_0$, and hence this parameter ($a$) increases with an increase in scan size. As we shall see in the next section, our previous results [20,25] and results of NEXAFS spectroscopic studies provide some validation for our model of frusta due to tilt variation.

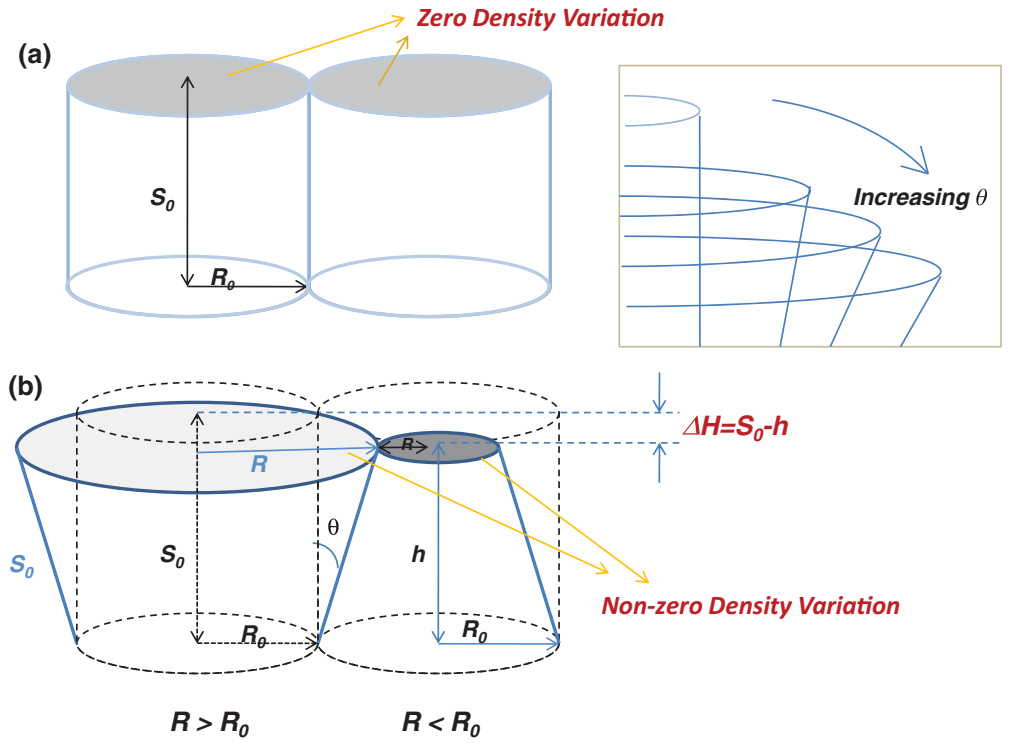


FIG. 5. (Color online) Model for explaining height and density variation in CoSt films. (a) Two cylinders of radius $R_0$ and density $\rho$ representing uniform distribution of untilted molecules. (b) Two frustums of unequal radii $R$ formed from the cylinders by molecular tilt showing density variation; height variation within the frustum of radius $R > R_0$ due to formation of concentric frustums (inset).

### B. Molecular orientation and tilt: NEXAFS measurements

In our previous reports, [20] we have shown that multilayers of CdSt are untilted with respect to the surface normal whereas the same for CoSt are oriented at an angle of 9°. These values refer to spatial averages along the $(x, y)$ direction. Hence they do not give information on the molecular orientation along this direction. In order to investigate the in-plane orientation of the molecules in CoSt films, NEXAFS spectra of 3 ML CoSt was carried out in transmission mode at the O $K$ edge. Data was taken for normal and grazing (20° with horizontal) incidence. The polarization in the plane normal to the beam was at 0°, 30°, 45°, 60°, and 90° for normal incidence, probing the in-plane orientation of the C-O bonds in the head groups, while the electric field polarizations for grazing incidence were at 0°, 15°, 30°, 45°, 60°, 75°, and 90°, probing the bond orientations normal to the film plane. The series of measurements showed no variation of the main absorption peaks with change in polarization angle (Fig. 7), signifying no net preferred in-plane orientation of head groups in the CoSt LB films. As the all-trans planes of the corresponding hydrocarbon chains are fixed, i.e., rigidly attached to the head group with respect to the surface normal [12], the tails do not have an overall preferred orientation with respect to surface normal. This indicates that for the CoSt system, the hydrocarbon tails are tilted in a radially symmetric manner with an average tilt of 9° giving rise to hemispherelike features in the phase images, with gradually increasing tilts from 0 to $\theta_{\max}$. The molecular tail tilt (Fig. 5) gives rise to both height and density variation, both becoming prominent only at small scan sizes, where the presence of pinholes do not mask this subtle variation. Moreover, as is clear from Fig. 5, the height variation due to individual molecular tilt (∼for a tilt of 9°) is much less pronounced than the density variation, and is consistent with the fact that the variation is more prominent in phase images than in height images.

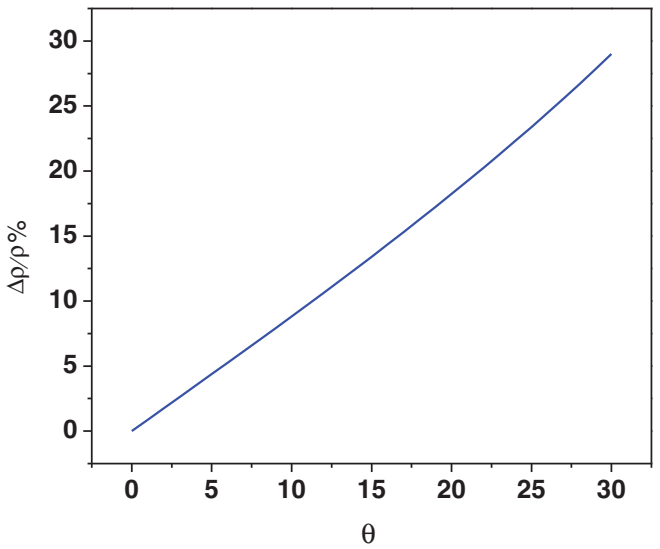


FIG. 6. (Color online) Graph of percentage density variation with molecular tilt.

We propose that this radially symmetric hydrocarbon tail tilt, although small (∼0°–18°) does give rise to a significant variation in density as is clearly brought out in our frusta model,

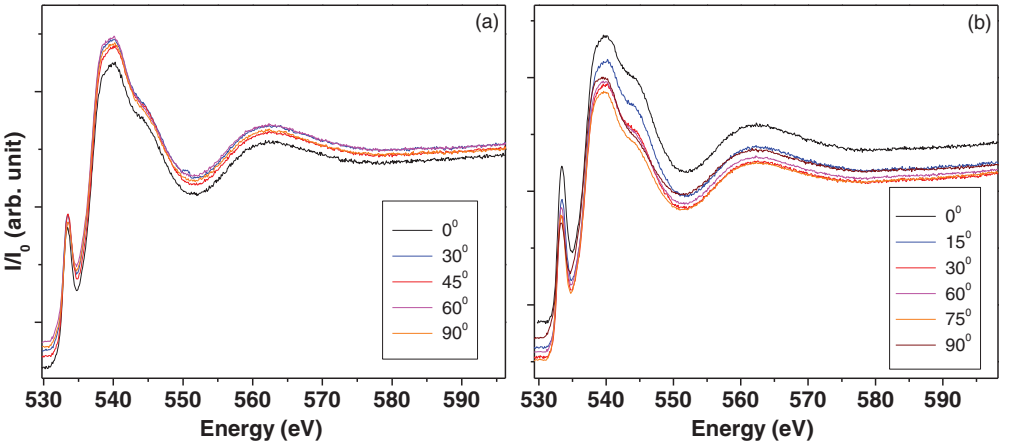


FIG. 7. (Color online) O $K$-edge NEXAFS spectra of 3 ML CoSt films at (a) normal and (b) grazing (20°) angles of incidence for different in-plane polarization angles.

while the same model results in a weak variation in height of the frusta. Thus the density variation caused by the variation in tail tilts are prominent in the AFM phase images but weak in the topographic images. This subtle height variation due to the variation in tilts also shows up as "taillike" features in the height-height correlation function. It is this random orientation of tails that allows "space filling" to occur along the in-plane direction in CoSt films reducing the pinholes in each layer as shown in the cartoon (Fig. 8). The connection between this reduction of the size of random desorption patches or pinholes with the emergence of dominant liquidlike height correlations is consistent with x-ray diffuse scattering studies [23]. In this connection, the $1/b$ parameter in the height-height correlation function assumes a significance as the "wavelength" of the correlated frusta.

The next question that comes to mind is regarding the presence of these liquidlike and solidlike features in the parent Langmuir monolayers of the metal-bearing amphiphiles. In order to investigate that, we have studied the metal-stearate monolayers at the air-water interface using BAM.

### C. Behavior of parent Langmuir monolayer: BAM measurements

Brewster angle microscopy (BAM) images of stearic acid monolayers (Fig. 9) with cadmium and cobalt ions in subphase show that the monolayers behave distinctly in the presence of these ions. The images correspond to monolayer decompression for two values of surface pressure, viz., $\pi = 30$ mN/m and $\pi = 5$ mN/m. With cadmium ions in subphase, stearic acid monolayer, when compressed (up to $\pi = 30$ mN/m), shows the formation of "crystallites" that remain unaffected when decompressed from $\pi = 30$ mN/m [Fig. 9(a)] to $\pi = 5$ mN/m [Fig. 9(b)]. The CdSt monolayer at 5 mN/m distinctly shows the presence of a monolayer on which these crystallites are formed. This is clear indication

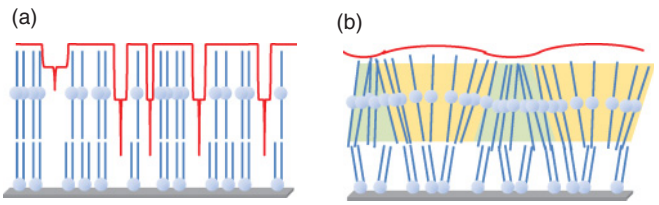


FIG. 8. (Color online) Cartoon showing (a) untilted hydrocarbon tails in CdSt and (b) radially symmetric tilt orientation of hydrocarbon tails in CoSt films in accordance with the frustum model.

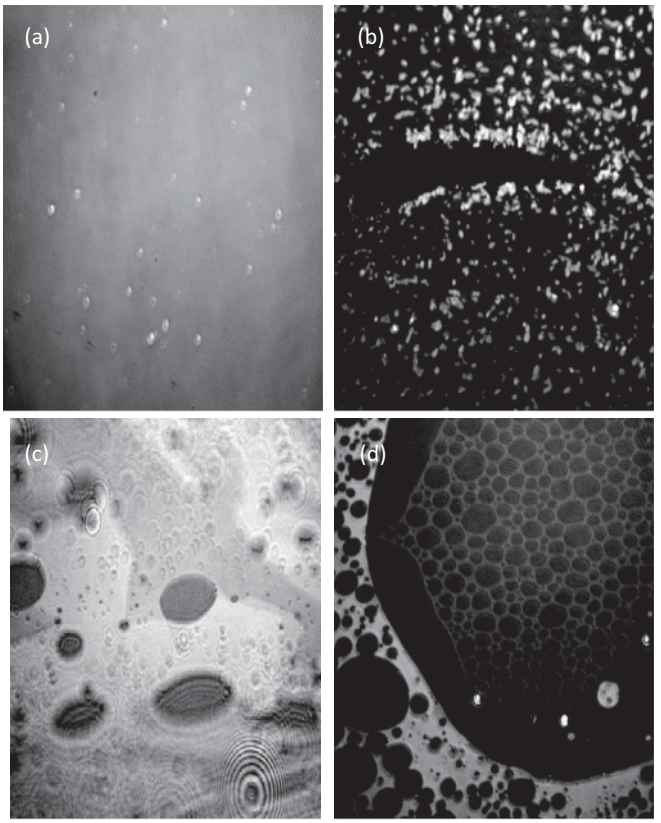


FIG. 9. (Color online) BAM images of stearic acid Langmuir monolayer with [(a),(b)] Cd and [(c),(d)] Co ions in subphase. The images are taken during decompression of the isotherm at [(a),(c)] 30 mN/m and [(b),(d)] 5 mN/m.

of CdSt multilayer formation at air-water interface and is consistent with our previous result [16], which shows that for CdSt the 1 ML film is not a true monolayer but is deposited as a multilayer. In the presence of cobalt ions, on the other hand, the monolayer "spreads out" gradually as $\pi$ changes from 30 mN/m [Fig. 9(c)] to 5 mN/m [Fig. 9(d)] and forms completely interconnected "soap-bubble-like" features on decompression. These aggregate continuously to form the monolayer on recompression. These decompression and recompression behaviors of Langmuir monolayers with cadmium and cobalt ions in subphase suggest, respectively, the essentially irreversible fracture of a solid and the reversible, interconnected-bubble features of a soapy liquid. It is thus evident that the CoSt system is inherently a more flexible system both at the air-water interface and the air-substrate interface and its liquidlike behavior arises probably due to the specific interaction of metal ion with the organic head group and not due to the transfer process. It is to be noted that the connection between this interaction and the liquidlike or solidlike features has been discussed for Langmuir-Blodgett multilayers in our previous works [16]. However, it has not been clarified for Langmuir monolayers and work toward that end is underway.

## IV. CONCLUSION

To conclude, atomic force microscopic studies of CdSt and CoSt Langmuir-Blodgett films clearly bring out the difference in their in-plane structures. The CdSt films, with a huge number of in-plane pinhole defects, exhibit self-affine behavior over a considerable scan range. On the other hand, the CoSt films, which are almost void of such in-plane defects, do not strictly follow the self-affine behavior. These films show deviation from self-affinity for small scan sizes and is pronounced for the trilayer film. The deviations probably suggest more of a liquidlike behavior and hence a much more flexible in-plane structure compared to CdSt films. The CoSt in-plane structure exhibits a smooth topography along with a gentle undulation, unlike the CdSt system, as seen from the AFM phase images. Such undulating topography in CoSt is probably achieved by the random orientation of the small tilts of adjacent hydrocarbon tails in a radially symmetric manner, as ascertained from NEXAFS spectoscopic studies. Thus in CoSt, tail orientations help fill up in-plane defects and give rise to excellent in-plane coverage. Investigation of the parent Langmuir monolayers of these metal-bearing amphiphiles show similar solidlike and liquidlike behavior at the air-water interface, thereby suggesting it to be arising from interaction of the metal ion with the organic moiety which remains largely unaffected by the transfer process.

## ACKNOWLEDGMENTS

The authors thank Professor Debabrata Ghose and Dr. Puneet Mishra for AFM measurements. Support from Department of Science and Technology for India-Italy POC [Project No. INT/ITALY(SYN-5CGM); Proposal No. 2006564] is acknowledged. S.M. acknowledges support by the Department of Atomic Energy, India.

[1] P. M. Chaikin and T. C. Lubensky, *Principles of Condensed Matter Physics* (Cambridge University Press, Cambridge, 1997).
[2] P. G. de Gennes and J. Prost, *The Physics of Liquid Crystals* (Oxford University Press, New York, 1995).
[3] V. M. Kaganer and E. B. Loginov, Phys. Rev. Lett. **71**, 2599 (1993).
[4] V. M. Kaganer and E. B. Loginov, Phys. Rev. E **51**, 2237 (1995).
[5] V. M. Kaganer, H. Mohwald, and P. Dutta, Rev. Mod. Phys. **71**, 779 (1999).
[6] D. Nelson, S. Weinberg, and T. Piran, *Statistical Mechanics of Membranes and Surfaces* (World Scientific Publishing Company, London, 2004).
[7] T. Aste, K. Y. Szeto, and W. Y. Tam, Phys. Rev. E **54**, 5482 (1996).
[8] M. K. Sanyal, S. K. Sinha, K. G. Huang, and B. M. Ocko, Phys. Rev. Lett. **66**, 628 (1991).
[9] J. Daillant and M. Alba, Rep. Prog. Phys. **63**, 1725 (2000).
[10] A. Datta, S. Kundu, M. K. Sanyal, J. Daillant, D. Luzet, C. Blot, and B. Struth, Phys. Rev. E **71**, 041604 (2005).
[11] J. Daillant, J. Pignat, S. Cantin, F. Perrot, S. Morac, and O. Konovalovd, Soft Matter **5**, 203 (2009).
[12] D. K. Schwartz, Surf. Sci. Rep. **27**, 241 (1997).
[13] J. K. Basu and M. K. Sanyal, Phys. Rev. Lett. **79**, 4617 (1997).
[14] J. K. Basu, S. Hazra, and M. K. Sanyal, Phys. Rev. Lett. **82**, 4675 (1999).
[15] A. Gibaud, N. Cowlam, G. Vignaud, and T. Richardson, Phys. Rev. Lett. **74**, 3205 (1995).
[16] S. Mukherjee, and A. Datta, Phys. Rev. E **83**, 041604 (2011).
[17] J. Stohr, *NEXAFS Spectroscopy* (Springer-Verlag, New York, 1996).
[18] S. Mukherjee and A. Datta, Appl. Surf. Sci. **256**, 380 (2009).
[19] I. Daruka and A. L. Barabási, Phys. Rev. Lett. **79**, 3708 (1997).
[20] S. Mukherjee, A. Datta, A. Giglia, N. Mahne, and S. Nannarone, Chem. Phys. Lett. **451**, 80 (2008).
[21] G. Palasantzas and J. Krim, Phys. Rev. B **48**, 2873 (1993).
[22] H.-N. Yang, Y.-P. Zhao, A. Chan, T.-M. Lu, and G.-C. Wang, Phys. Rev. B **56**, 4224 (1997).
[23] M. Li, X. H. Li, L. Huang, Q. J. Jia, W. L. Zheng, and Z. H. Mai, Europhys. Lett. **64**, 385 (2003).
[24] G. Palasantzas, Solid State Commun. **100**, 705 (1996).
[25] S. Mukherjee, A. Datta, A. Giglia, N. Mahne, and S. Nannarone, Langmuir **25**, 3519 (2009).